Advantages and Risks in Increasing Cyclone Separator Length

A. C. Hoffmann
Dept. of Physics, University of Bergen, 5007 Bergen, Norway

M. de Groot and W. Peng
Dept. of Chemical Engineering, University of Groningen, 9747 AG Groningen, The Netherlands

H. W. A. Dries and J. Kater
Shell Global Solutions International B.V., 1030 BN Amsterdam, The Netherlands

The effect of cyclone length on separation efficiency and pressure drop has been investigated experimentally and theoretically by varying the length of the cylindrical segment of a cylinder-on-cone cyclone. Experimental results based on cyclone lengths from 2.65 to 6.15 cyclone diameters showed a marked improvement in cyclone performance with increasing length up to 5.5 cyclone diameters; beyond this length the separation efficiency was dramatically reduced. Experimental data agreed well with the predictions of a range of models and CFD simulations. This helps to assess the benefit of prolonging a given cyclone. The physical mechanisms behind the observed trends are elucidated. The dramatic fall in separation performance for the longest length was caused by the "natural turning" phenomenon.

Introduction and Background

Cyclones are the most widely used dedusting device. Among many other applications, they are an essential component in fluid catalytic cracking (FCC) units, which convert heavy feeds into lighter products by cracking large molecules into smaller ones over a solid catalyst. Dedusting or demisting with cyclones or swirl tubes is vastly superior to other methods in terms of investment and operating costs, ease of operation, and space requirements.

When faced with the need to meet more stringent emission requirements, both for environmental protection and for safeguarding downstream equipment, it is preferable to improve cyclone performance rather than having to resort to alternative units. One option for this is to make the cyclone separation space longer, which most models agree will improve performance.

This study aims to quantify this improvement and to explain it in light of the concepts behind the cyclone models and the flow pattern in the separation space. The goal is to help in assessing whether prolonging cyclone body length is worthwhile in a given context.

The two performance indicators used are the pressure drop and the particle separation efficiency. The latter is normally expressed as a "grade-efficiency curve": a graph of the collection efficiency against the particle size.

Correspondence concerning this article should be addressed to A. C. Hoffmann.

Effect of Cyclone Length in the Literature: Model Predictions and Experimental Studies

Two basic concepts have been proposed in the research literature for modeling cyclone separation performance. They are illustrated in Figure 1.

One concept is to balance the centrifugal force against drag in the surface *CS*, assumed to be the boundary between the outer region of downward flow and the inner one of upward flow. The outwardly directed centrifugal force is proportional to the particle mass, and thus the diameter cubed, while the (Stokesian) drag due to the inwardly directed gas flow across CS is proportional to the diameter to the first power. Larger particles are therefore better separated. For the "critical" or "cut" diameter of the cyclone the two forces balance.

The other concept is to consider whether particles will reach the wall, where they are assumed collected, before the bottom of the cyclone. Also in this type of model, the tangential gas velocity is assumed to be axially uniform, and the radial gas velocity is ignored when calculating the rate of particle migration to the wall. The cut diameter is the particle

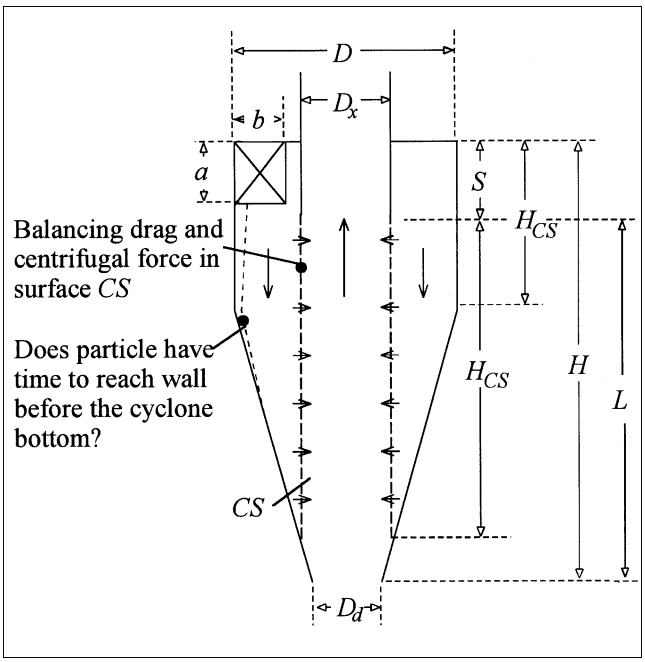

Figure 1. Cyclone showing cyclone dimensions and concepts behind models for separation performance.

that will just reach the wall when injected in the middle of the inlet.

In spite of the very different underlying concepts, both types of model are highly successful in predicting cut diameters. Other, later, models consider migration to the wall with radial mixing (Leith and Licht, 1972; Clift et al., 1991) or are hybrids between the two concepts (Mothes and Löffler, 1985; Dietz, 1981; see also Clift et al, 1991), considering both wall migration and transport at *CS*.

The classic model according to the force-balance concept is the model of Barth (1956), which predicts for the critical particle diameter d_{p50}:

$$d_{p50} = \frac{1}{v_{\theta,CS}} \cdot \left(\frac{18 \cdot \mu_g \cdot v_{r,CS} \cdot R_{CS}}{(\rho_p - \rho_g)} \right)^{1/2} \text{ with } v_{r,CS} = \frac{\phi_v}{\pi \cdot D_x \cdot H_{CS}}, \tag{1}$$

where (v_r, v_θ, v_z) are the radial, tangential, and axial velocity components, respectively; μ is the viscosity, ρ the density, subscripts p and g refer to the particle and gas, respectively, and $v_{r,CS}$ and $v_{\theta,CS}$ are the radial and tangential gas velocity in the surface *CS* that has radius R_{CS} and extends through the separation space from the vortex finder wall. These velocities are assumed uniform, which gives the expression for $v_{r,CS}$ in Eq. 1. The volumetric gas flow rate is ϕ_v. The rest of the symbols for the geometrical parameters are shown in Figure 1.

The wall migration concept was used by Rietema (1958). Rietema relates v_θ to the cyclone pressure drop to end up with an expression for cyclone cut size in terms of the pressure drop Δp:

$$\frac{d_{p50}^2(\rho_p - \rho_g)}{\mu_g} H \frac{\Delta p}{\rho_g \phi_v} = 3.5. \tag{2}$$

Examining these equations shows that if v_θ and Δp remain constant with increasing H, both concepts predict a decrease in d_{p50} according to $H^{-0.5}$. The physical reasons are the decreased inward drag on the particle in the model of Barth, and the increased time available for a given particle to reach the wall in the model of Rietema.

However, some models predict a decrease in v_θ with increasing cyclone length. Barth (1956) and Meissner and Löffler (1984) found the radial profile of v_θ by carrying out moment-of-momentum (also called angular momentum) balances on the gas, taking into account frictional losses in the separation space. They predicted a decrease in v_θ with increasing H due to the increased friction at the larger cyclone wall. Another model for v_θ is the simple n-law: $v_\theta = (C/r^n)$, with C a constant. This is an adaptation of the loss-free vortex law, for which $n = 1$. In cyclones, n is normally taken as 0.7 or 0.8. To reflect a change in the swirl velocity with cyclone length, n can be made a function of length empirically.

Also some models predict a decrease in Δp with increasing H, as we shall see below. Inspecting Eqs. 1 and 2, we see that these predicted dependencies of v_θ and Δp on H both work against the explicit effect of H on d_{p50}, and we therefore cannot *a priori* be certain of the effect of increasing H on d_{p50} on the basis of an inspection of the model equations, although we expect a decrease.

We now return to the tangential velocity in the cyclone, v_θ. As mentioned, all of the models assume that v_θ is uniform axially. However, when studying the effect of cyclone length, we should also focus on the development in the flow pattern as we move down the cyclone separation space, away from the inlet where the driving force for the swirl is.

There are few details available about this. Alexander (1949) found that the vortex suddenly and spontaneously stops somewhere low in the cyclone. He called the distance from the bottom of the vortex finder to the position of this end of the vortex the "natural vortex length," L_n, and found empirically:

$$\frac{L_n}{D} = 2.3 \frac{D_x}{D} \left(\frac{D^2}{ab} \right)^{1/3}. \tag{3}$$

Also Zhongli et al. (1991) proposed an expression for L_n involving the same groups, but with a variation in L_n with both of the groups opposite to that in Eq. 3.

It is often stated that if cyclones are built longer than the natural length, the space under the vortex end is wasted and ineffective in the separation. Some models use the natural vortex length rather than the physical one as a measure of cyclone length. Hoffmann et al. (1995) found, however, that if the vortex ended in the conical part of the cyclone, the fall in separation performance was far greater than one would expect simply from the reduction in effective length. They also found the natural length to depend on the solid loading, probably due to a changing apparent wall roughness. Ito et

al. (1980) considered the variation in the swirl axially and found that both the decay of the swirl intensity and the natural vortex length depend on the length of the cyclone. This was confirmed by Akiyama and Marui (1989).

Finally, we mention models for cyclone pressure drop. Most are purely empirical. They often incorporate only the dimension of the gas inlet and outlet (such as Casal and Martinez, 1983; Shepherd and Lapple, 1939), and therefore do not predict any change in pressure drop with body length.

Two exceptions are the models of Stairmand and Barth. Stairmand (1949) calculated the velocity distribution in the cyclone from a moment of momentum balance, and then estimated the pressure drop as entrance and exit losses combined with the loss of static head in the vortex, somewhat in line with the discussion of cyclone pressure drop below. Stairmand's model is worked out in a compact form in Iozia and Leith (1989).

The model of Barth (1956; see also Muschelknautz, 1970) calculates the pressure drop from the dissipative loss in the cyclone inlet, body, and vortex finder. The latter depends on the swirl velocity in the center of the cyclone, which again depends on the frictional loss in the cyclone body. The loss in the vortex finder is greater than the other two by an order of magnitude, and it is given as

$$\frac{\Delta P}{\left(1/2\rho\langle v_{ax}\rangle^2\right)} = \left(\frac{v_{\theta,CS}}{\langle v_{ax}\rangle}\right)^2 + K\left(\frac{v_{\theta,CS}}{\langle v_{ax}\rangle}\right)^{4/3} \qquad (4)$$

where $\langle v_{ax}\rangle$ is the cross-sectional mean axial gas velocity in the gas outlet. Clearly, if $v_{\theta,CS}$ decreases with increasing H due to an increase in frictional loss in the cyclone body, so does the pressure drop according to Eq. 4. K takes the values of 3.41 and 4.4 for vortex finders with smooth and sharp edges, respectively. Muschelknautz (1970) proposes a slight change to Eq. 4, but this does not change the predictions very much. On the other hand, the friction factors given by Muschelknautz for calculating the wall frictional loss are probably more realistic than those of Barth.

Computational fluid dynamics (CFD) is suitable for predicting all aspects of cyclone performance. The problems of correctly simulating a highly swirling, confined flow are well known, and will not be discussed here. The CFD package used to elucidate the effect of cyclone length here is two-dimensional (2-D) axisymmetric. It uses a skew upwind differencing scheme (SUDS). This scheme is, together with the QUICK scheme, considered best for swirling flows with significant cross-grid velocity components. The turbulence model is a hybrid between an algebraic stress model and a full Reynolds stress model (Boysan et al., 1986). Recent research (Hoekstra et al., 1999a,b) shows that the error arising from not including 3-D effects when simulating the flow in cyclones is small. The separation efficiency was determined using Lagrangian particle tracking in the precalculated flow field. This is allowed, since the solid loading was low in the experiments, so that the particles have only little effect on the gas flow field.

We turn now to the few experimental investigations of the effect of cyclone length. Iozia and Leith (1989) studied cyclone configurations with body lengths of $3D$ and $5D$. The overall efficiency and pressure drop were not presented. They mainly studied the tangential velocity profile in terms of maximum tangential velocity and the width of the region inside this maximum: the core. They found that the maximum tangential velocity decreases with cyclone length, while length has little effect on the core width. The work gives no clue as to an optimal cyclone length. It appears from their article that the vortex end was in the dust hopper below the cyclone.

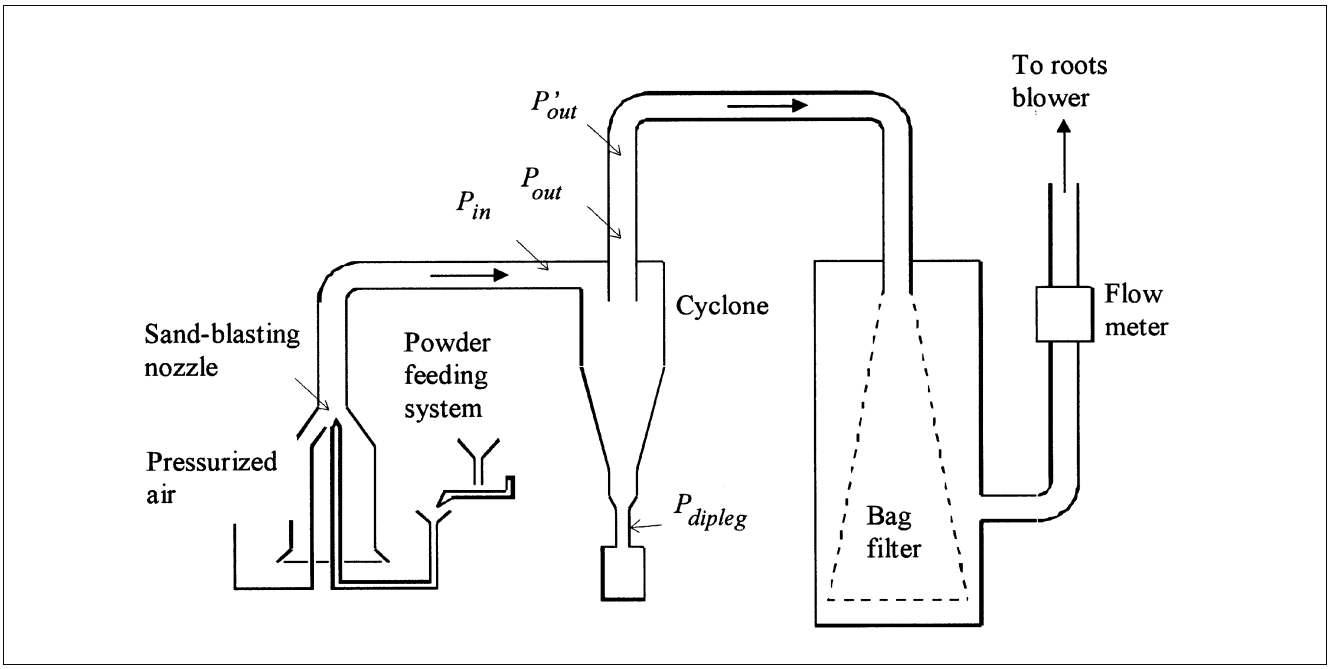

Figure 2. Experimental equipment.

A patent application of MacLean et al. (1978) claims a design of cyclone with an optimal body length of:

$$\frac{L}{D} = -1.09\left(\frac{O}{I}\right) + 4.49, \tag{5}$$

where O and I are the cross-sectional areas of the outlet and inlet, respectively, and L is shown in Figure 1. The patent claims the advantages of better separation and less wear, but it is not stated how this optimal cyclone length was found.

This study aims to quantify the effect of cyclone length on performance and explain it physically, in order to help in assessing whether prolonging cyclone body length is an attractive option for augmenting cyclone performance.

Experimental Studies

The tests were executed using a Perspex model. The test powder had a size distribution such that the separation performance in the test rig with air under ambient conditions was comparable to that of the industrial cyclones under plant conditions. The particle size ranged from 0.3 μm to 60 μm, with a volume mean of 3.65 μm and a density of 2730 kg/m^3.

The cyclone length, H, was varied in seven steps in the range 0.67 to 1.37 m by varying the length of the cylindrical section.

The performance of these configurations was assessed by determining:

- The percentage overall efficiency (η)
- The pressure drop inlet to gas outlet (ΔP)
- The pressure drop inlet to dust outlet and in some cases, the grade efficiency.

Test rig

A diagram of the experimental equipment is shown in Figure 2. The dust-laden air is drawn through the system by a roots blower at the exit of the rig. The gas is charged with test dust at the entrance to the system using a so-called sand-blasting nozzle. In the cyclone most of the particles are separated from the gas and collected in a hopper underneath. Having passed the cyclone, the gas flows through a large, membrane-coated filter bag, which removes all the remaining dust particles by surface filtration. Under the filter bag, a circular steel plate is fixed, in which all the removed particles can be collected. The filter bag with the plate can be weighed *in situ*.

The cyclone dimensions are (symbols in Figure 1): $D =$ 0.200 m, $D_x = 0.065$ m, $D_d = 0.110$ m, $S = 0.140$ m, $a = 0.114$ m, $b = 0.050$ m, and $H_c = 0.410$ m. It is equipped with extra cylindrical sections so that the length of the cylindrical segment of the body can be varied between 0.260 and 0.960 m. Figure 3 gives a visual impression of the range of cyclone lengths tested.

Experimental program

A total of 19 experiments were executed, some of which were repeats. During each experiment the overall efficiency was determined, and the pressure at each of the measuring points indicated in Figure 2 were recorded a number of times. Samples from the lost and collected dust fractions were obtained and reduced using a spinning riffler for particle-size analysis in a Joyce-Loebl centrifuge.

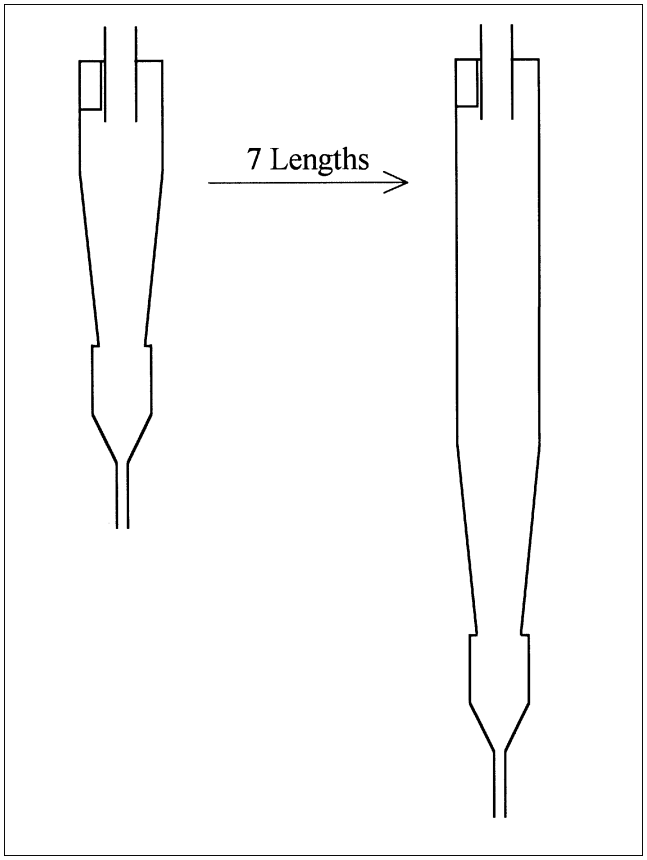

Figure 3. Range of cyclone lengths tested.

We calculate the dimensionless length of the working part of the cyclone as

$$\frac{L}{D} = \frac{H - S}{D}, \tag{6}$$

and tested the following values of L/D: 2.65, 3.15, 3.65, 4.15, 4.65, 5.65, and 6.15.

For all the tests, the experimental conditions were the same:

- The dust load was around 1.6 or 1.7 g dust/m^3 gas.
- The volumetric flow rate was approximately 390 m^3/h, giving an inlet velocity of 19 m/s.

Results and Discussion

Separation efficiency

The overall experimental efficiencies are shown in Figure 4. A clear trend of increasing separation efficiency is seen. However, the efficiency suddenly becomes much poorer when the length is increased to 1.37 m, corresponding to $L/D =$ 6.15.

In order to compare with the predictions of the models, the overall efficiencies must be converted into a cyclone cut size. If we know the cumulative volumetric size distribution

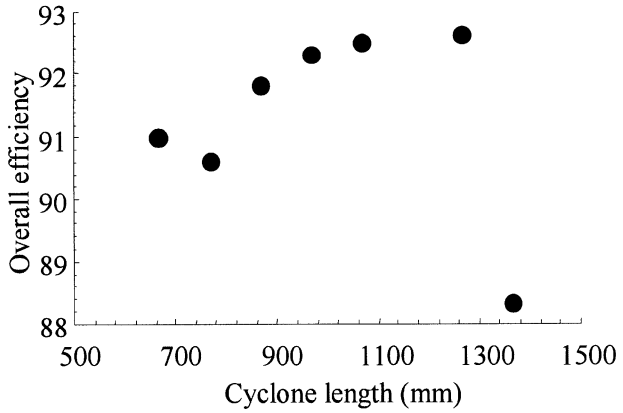

Figure 4. Experimental results of overall efficiency vs. cyclone length.

of the feed,

$$F(d_p) = \int_0^{d_p} f(x)\, d(x), \tag{7}$$

and we assume that all material below the cut size d_{p50} is lost and all material above is collected, we can calculate d_{p50} from

$$F(d_{p,50}) = 1 - \eta_{\text{overall}}. \tag{8}$$

For our test powder, $F(d_p)$ is well approximated by a log-normal distribution, that is,

$$f(d_p) = \frac{1}{d_p}\frac{1}{\sigma\sqrt{2\pi}} \cdot \exp\left(-\frac{\left(\ln d_p - \langle z \rangle\right)^2}{2\sigma^2}\right), \tag{9}$$

with a mean $\langle z \rangle$ of 1.3 (d_p is measured in μm) and a spread σ of 1.0. The results of calculating the cut sizes from Eqs. 8 and 9 are shown as open circles in Figure 5. In two cases, the grade-efficiency curves were generated on the basis of size analyses of the lost and collected dust fractions, and the cut size read off as the size corresponding to 50% capture. This is shown as the black squares in the figure.

Figure 5 also shows the predictions of selected models. As is so often the case, the classic models of Barth and Rietema

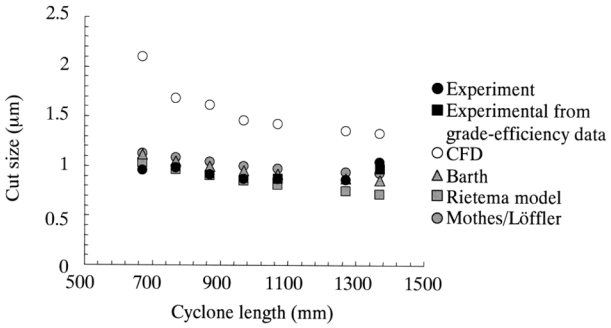

Figure 5. Cut size as a function of cyclone length.

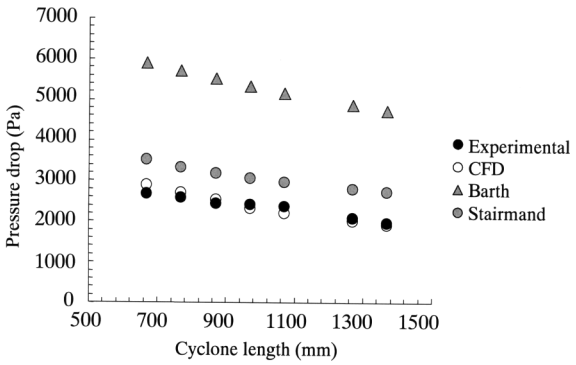

Figure 6. Pressure drop as a function of cyclone length.

agree closely in spite of the very different concepts behind them. Also the model of Mothes and Löffler agree with the two others in predicting a decreasing cut size with increasing cyclone length in this range. The improvement is less at the longer lengths. The predictions of the models are in good agreement with experiment.

The Shepherd and Lapple pressure-drop model, in which Δp does not vary with H, was used to find Δp in the Rietema model, Eq. 2. When pressure-drop models that reflect the decrease in Δp with increasing H were tried, almost the same trend as in Figure 5 was found.

The y-axis is expanded to show all the results and predictions, and this underemphasizes the improvement with length, which we saw experimentally. Using cyclones with L/D of 4.65 and 5.65 gave about 20% reduction in *emission* compared with 2.65 and 3.15.

The CFD predictions of the cut size are not so good. This is surprising, since this same package has predicted cut sizes in other cyclones very successfully. The trend in the CFD predictions is seen to be the same as in the models.

None of the predictions reflect the dramatic decrease in efficiency for the longest length. Below, we show that this decrease is due to the natural vortex turning phenomenon.

Pressure drop

Figure 6 shows the pressure drop inlet to outlet. The pressure drop decreases significantly with increasing length, falling by about one-third from the shortest to the longest length.

Determining the pressure in the outlet of cyclones is complicated by the swirl present there:

- Dynamic pressure is stored in the swirling motion.
- The static pressure is not uniform in the swirling flow, but highest at the wall.

In this work, the static pressure in the outlet was measured at the wall. Hoffmann et al. (1992) found that the static pressure in the outlet of a cyclone is an almost linear function of the radius. They showed that in this case the static wall pressure is equal to the cross-sectional mean of the static pressure plus the dynamic pressure stored in the swirling motion: $(p + 1/2\,\rho_g v_\theta^2)$, which is also the mean static pressure as it would have been after an ideal rectifier. Since the axial velocity in the gas exit is fairly uniform, the cross-sectional means can be taken as the mean in the flowing gas. We stress that

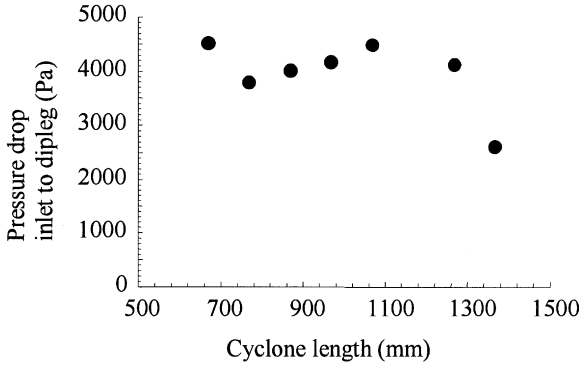

Figure 7. Pressure drop inlet to dipleg as a function of cyclone length.

this is by no means an inherent necessity, but rather a *coincidental feature* of the flow, which follows from the observed fact that the static pressure just downstream of the cyclone is an almost linear function of the radial position.

Barth's model can be seen to predict the right trend in the pressure drop, but somewhat higher absolute values. The predictions of the Stairmand model and the CFD simulations appear to be in excellent agreement with experiment, both in terms of absolute values and trend with cyclone length. However, see also the discussion of the pressure drop later in this article.

Figure 7 shows the pressure drop inlet to dipleg. The higher this pressure drop, the more severe the vacuum drawn in the dust box. For the longest length the vacuum in the dust box falls dramatically.

Figure 8 shows the pressure drop in the downstream tubing ($P_{out} - P'_{out}$). This pressure drop falls with increasing cyclone length.

The preceding results show that the cyclone performance improves with an increasing body length. However, extending the cyclone length beyond $L/D = 5.5$ lead to significantly lower efficiencies. We have mentioned that this can be attributed to the natural turning phenomenon of the vortex. This is supported below.

Visual observations under the cyclone

In the sections below the cyclone, a strong spiralling flow

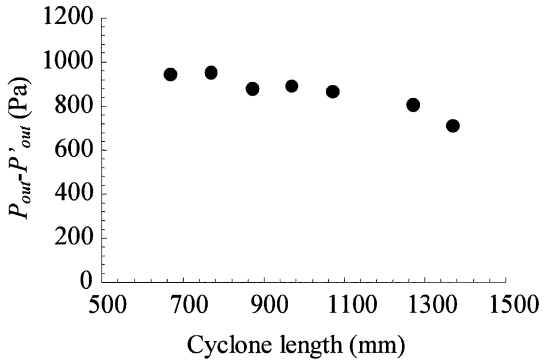

Figure 8. Pressure drop in the downstream tubing as a function of cyclone length.

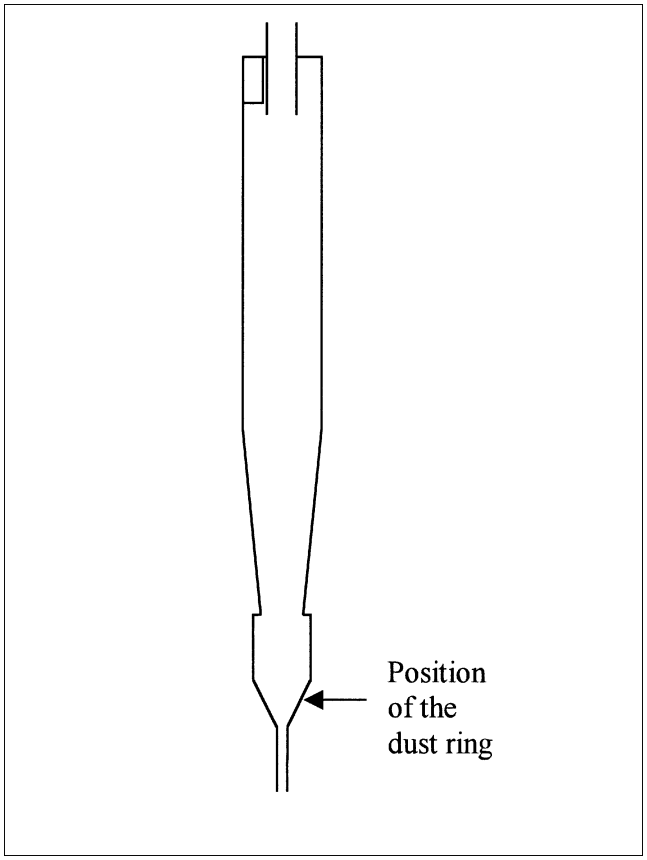

Figure 9. Arrow indicates the position at which the turning of the vortex was observed in the longest cyclone.

of gas and particles was observed. No influence of cyclone length was visible until the maximum.

At the longest length, a dust ring was repeatedly observed at the wall of the conical section under the cyclone proper (see Figure 9) and the pressure drop $P_{in} - P_{\text{dipleg}}$ (Figure 2) decreased enormously. Under the dust ring the transport of particles toward the collection room was obviously bad. Initially the situation was unstable, but after half an hour the situation stabilized: the pressure of the dust box remained low and the dust ring became a permanent feature positioned on the conical wall of the dust hopper. During the experiment the dust ring gained a thickness of almost half a centimeter and the funnel underneath the ring was partly filled with powder. In the past this ring has been observed to signify the natural turning point of the vortex. When we compare the dramatic decrease in the separation efficiency here with the results of Hoffmann et al. (1995), it would seem that the vortex turning on a conical wall causes the separation efficiency of the cyclone to collapse, probably due to increased reintrainment.

Further Discussion

In this section we discuss the performance of the cyclone compared to other centrifugal gas cleaning equipment. After

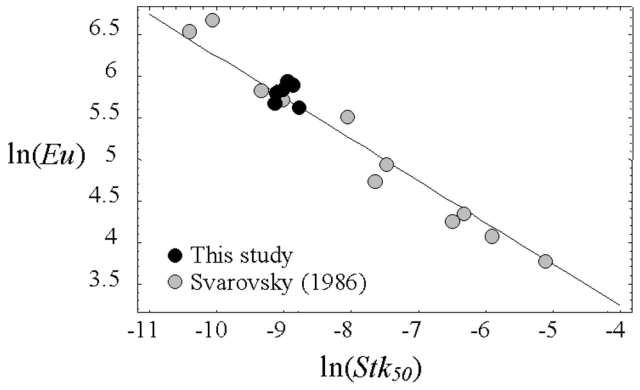

Figure 10. ln(*Eu*) plotted against ln(Stk_{50}) for this cyclone vs. data of Svarovsky (1986).

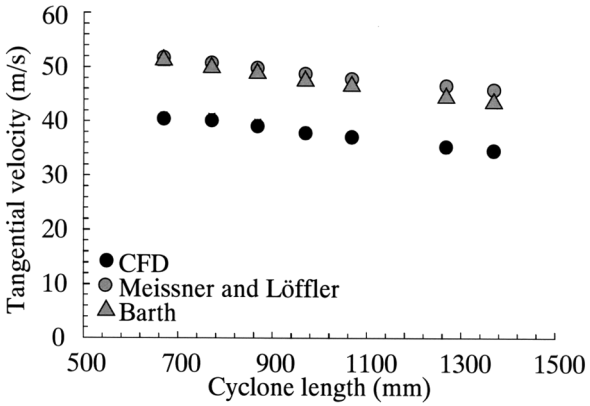

Figure 11. $v_{\theta,CS}$ as a function of cyclone length.
For CFD $v_{\theta,CS}$ is taken as the tangential velocity just under the lip of the vortex finder.

this, the issue of the cyclone pressure drop, which has emerged as an important effect of changing the cyclone length, is elucidated. Finally, the drop in efficiency for the longest cyclone is discussed further as an effect of the natural turning phenomenon.

The overall performance of the cyclone in context

Svarovsky (1986) gives the following expression for the performance of gas cyclones:

$$Eu\sqrt{Stk_{50}} = \sqrt{12}\,, \tag{10}$$

with

$$Eu \equiv \frac{\Delta P}{\frac{1}{2}\rho v_a^2} \quad \text{and} \quad Stk_{50} \equiv \frac{(\rho_p - \rho_g) d_{p50}^2 v_a}{18\mu_g D}. \tag{11}$$

Here v_a is the cross-sectional mean axial gas velocity in the cyclone body, μ_g is the gas viscosity, and ρ_p is the particle density. The experimental results are shown in a plot of ln(Eu) versus ln(Stk_{50}) in Figure 10 and, in support of Eq. 10, compared with the results presented by Svarovsky.

The results fall close to the line representing Eq. 10, so the cyclone obviously works well. As it is made longer, we move downward in the diagram and a little to the left, reflecting the improvement in pressure drop and efficiency. The point corresponding to the longest cyclone falls to the right of the rest of the points.

Cyclone pressure drop

The effect of cyclone length in decreasing the pressure drop is probably similar in nature to the effect of increasing the solids loading (Hoffmann et al., 1991). An increase in solids loading leads to an increase in apparent friction factor at the wall, and therefore a decrease in swirl intensity and cyclone pressure drop. Also when the cyclone length in increased, the wall friction increases, which can be expected to reduce the swirl intensity.

We can confirm this reduction in swirl intensity by studying the results of model predictions and CFD simulations. Figure 11 shows predictions for the swirl velocity in *CS* $v_{\theta,CS}$ as a function of cyclone length; $v_{\theta CS}$ is predicted to decrease with increasing cyclone length, and the predictions of all three models agree well.

It can seem contraintuitive that the cyclone pressure drop should decrease with increasing body length and solids loading, since more wall area and more solids bouncing and rolling on the wall gives rise to more friction, and therefore, one might expect, to more dissipation.

That the pressure drop should nevertheless decrease can be visualized in the following way. As gas moves inward in the cyclone body, it is accelerated in accordance with the principle of conservation of moment of momentum. Also its static pressure decreases. We can say that the swirl transforms static pressure into dynamic pressure. The more intense the swirling motion, the more efficient this conversion, and the lower the central static pressure with which the gas enters the vortex finder. In the vortex finder we can assume (in the absence of a rectifying device) that the energy stored in the swirling component of the motion is dissipated without much recovery of static pressure.

Now consider two extremes for the flow pattern in the cyclone body: (1) swirl with a very low loss, and (2) almost complete dissipation of the swirl. By low-loss swirl, a large amount of static pressure is transformed to dynamic pressure. If the inlet velocity is 15 m/s, the tangential velocity in the center is about 45 m/s. Dynamic pressure of the order of ($1/2\ \rho_g\ 45^2$) Pa is then dissipated in the vortex finder per unit volume of gas. At the other extreme, with a lot of friction at the wall, robbing the inlet jet of all its dynamic pressure (visualize this by a baffle placed on the wall in front of the inlet), dynamic pressure of the order of ($1/2\ \rho_g\ 15^2$) Pa is dissipated per unit volume of gas, which is an order of magnitude less. In this latter case, the air will enter the vortex finder at a much higher static pressure with very little swirling motion, and the rate of dissipation in the vortex finder will be relatively small.

To further study this, the average static pressure and the dynamic pressure stored in the swirling motion were calculated for the gas entering the vortex finder, based on CFD

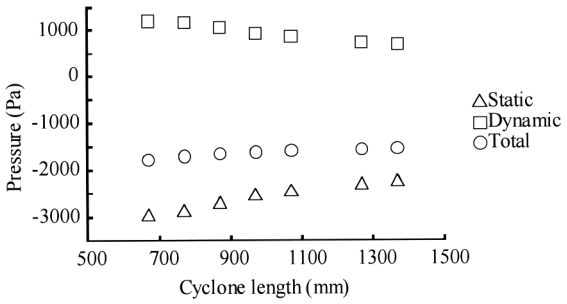

Figure 12. Static (relative to the wall pressure at the inlet) and dynamic pressures in the gas as it enters the vortex finder, calculated from CFD simulations.

simulations. This was done the discrete equivalent of:

$$\langle f \rangle = \frac{\int_0^R f(r) v_{ax}(r) 2\pi r dr}{\int_0^R v_{ax}(r) 2\pi r dr}, \qquad (12)$$

where v_{ax} is the axial velocity, R is the radius of the vortex finder, and $f(r)$ is, for the static pressure, $P(r)$, and, for the dynamic pressure in the swirl, $1/2\ \rho v_{\theta x}^2(r)$, with $v_{\theta x}$ the tangential velocity.

The result is shown in Figure 12. It shows the static pressure increasing and the dynamic pressure decreasing with increasing cyclone length. The total pressure increases marginally with increasing length, although we would have expected a marginal decrease. This may be due to inaccuracies in the CFD flow field, or in the calculations.

A second issue related to cyclone pressure drop is the swirl in the vortex finder, which makes the static pressure nonuniform radially. Calculations based on the CFD results show that pressure drops some 20% higher would have been recorded if the cross-sectional average static pressure at the outlet had been used rather than that at the wall. We found that the cross-sectional average does not differ much from the mean in the flowing gas, as calculated from Eq. 12.

Figure 12 shows that a considerable amount of dynamic pressure is still present at this point. As mentioned, the Hoffmann et al.'s results (1992) indicate that the static pressure at the wall is close to the cross-sectional mean of the total pressure.

The models of Barth and Stairmand give the pressure drop *after complete dissipation* of the swirling motion. At the point where this dissipation is complete, we can expect the static pressure to be slightly below the average static pressure at our measuring point. The discussion in the previous paragraph leads us to expect that the measured pressure drops would then be 20–30% higher than those shown in Figure 6. This explains much of the difference between the Barth's model, on the one hand, and the measurements and CFD simulations, on the other.

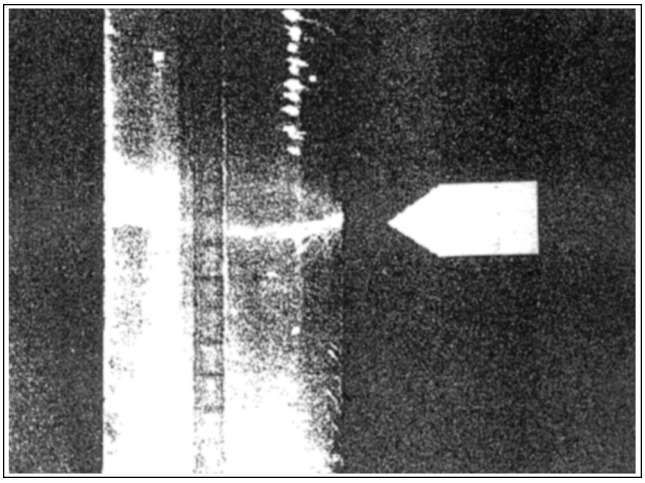

Figure 13. Ring formation at the end of the vortex in a cylindrical section underneath a cylinder-on-cone cyclone.

From Hoffmann et al. (1995).

Natural turning length

As mentioned, the sudden drop in efficiency for the longest length is due to the natural turning of the vortex. Past work by the authors with a cyclone with a tubular section attached to the dust exit showed that:

- The end of the vortex could clearly be seen, and could be visualized in different ways, for instance, as a dust ring. Figure 13 shows a ring at the end of the vortex formed in a liquid on the wall of a cylindrical section below a gas cyclone.
- The cyclone performed well when the vortex end was positioned in the tubular section.
- The separation performance dropped significantly and became erratic when the vortex end was in the conical section of the cyclone itself.

The nature of the end of the vortex is not yet known. This issue was discussed in Hoffmann et al. (1995), where the authors concluded that their observations would be consistent with an axisymmetric vortex turning point. Later experiments have been performed in water models, where the cyclone abruptly ends in a dust-collection hopper. These experiments showed that the vortex can bend and the vortex core attach to the lower edge of the cyclone wall, where it moves around rapidly ("vortex precession"). However, these water experiments have not yet succeeded in creating a vortex end on the wall itself, only on the lower edge.

In the present series of experiments the end of the vortex was observed for the longest length in the conical section below the cyclone proper, indicated with an arrow in Figure 9.

Two models have been proposed for the natural vortex length, as mentioned in the Introduction: the relations of Alexander (1949) and of Zhongli et al. (1991). The Alexander relation predicts $L_n = 0.326$ m, which is shorter than the shortest cyclone, and the model of Zhongli et al. predicts $L_n = 2.22$ m, which is longer than the longest one. As mentioned earlier the trend in L_n with the geometrical parameters is exactly opposite between the two relations. Although the absolute value of Zhongli et al. appears closer to the experiment, the variation of L_n (at least with D_x/D) is, in our

experience, more plausible in Alexander's relation. None of the two predict the strong variation with solid loading or the influence of the geometry that we have observed in the past (Hoffmann et al., 1995).

Büttner (1999) claims that the vortex length increases very strongly with the cyclone Reynolds number; so strongly, in fact, that in cyclones larger than a few centimeters in diameter there should be no problem with the natural turning of the vortex. Our results may support that the vortex length increases with Reynolds number, but not as strongly as Büttner claims.

We note MacLean et al.'s patent application (1978), where an optimal length is expressed in Eq. 5. For our geometry the optimal length should therefore be: $L/D = 3.67$, while experimentally the performance improved until $L/D = 5.65$. In light of earlier experience—that wall roughness, which can also be caused by powder, destabilizes the vortex—MacLean et al.'s design criterion seems quite reasonable. A key to optimizing the cyclone length further for a given function, leading to better performance, is to formulate a better model for the natural turning length.

It is interesting to note the variation in the vacuum drawn in the dust box (Figure 7). In the case where the vortex naturally turns above the dust box, it is enormously reduced. In this case, the natural end of the vortex was just above the dust box, and it is likely that if it had been higher, the vacuum would have been even lower.

Conclusions

The cyclone works well (Figure 9). Its performance improves with increasing body length. The separation efficiency also improves, but the most important effect is a fall in pressure drop. However, we found an optimal cyclone length: lengthening the cyclone to more than $L/D = 5.65$ led to dramatically lower separation efficiency.

Some models and the CFD package used performed well in predicting the effect of cyclone length on separation performance and pressure drop. The drop in efficiency for the longest cyclone is almost certainly due to the vortex turning above the dust box. The turning of the vortex above the dust box reduces the vacuum drawn in the box. Lengthening the cyclone body improves performance so much that it is commercially interesting, but better models for the natural vortex length are necessary in order to utilize this design aspect with confidence.

In this article we have not looked at the influence of varying the cylinder/cone ratio for a given overall length. Although the conical shape definitely influences the flow pattern in the cyclone, we are of the opinion that the effects we are seeing here are consequences of differences in the wall area and in the height of *CS*. We would therefore expect similar effects if the cylinder/cone ratio was changed within limits, for instance, by achieving the longer cyclones by using longer conical sections rather than longer cylindrical sections.

Literature Cited

Akiyama, T., and T. Marui, "Dust Collection Efficiency of a Straight-Through Cyclone; Effects of Duct Length, Guide Vanes and Nozzle Angle for Secondary Rotational Air Flow," *Powder Technol.*, **58**, 181 (1989).

Alexander, R. Mck., "Fundamentals of Cyclone Design and Operation," *Proc. Austral. Inst. Min. Met.,* **203**, 152 (1949).

Barth, W., "Berechnung und Auslegung von Zyklonabscheidern auf Grund neuerer Unterscuhungen," *Brennst.-Wärme-Kraft*, **8**, 1, (1956).

Boysan, F., J. Swithenbank, and W. H. Ayers, "Mathematical Modelling of Gas-Particle Flows in Cyclone Separators," *Encyclopedia of Fluid Mechanics*, Vol. 4, Cheremisinof, ed., Gulf Pub., Houston, p. 1307 (1986).

Büttner, H., "Dimensionless Representation of Particle Separation Characteristic of Cyclones," *J. Aerosol Sci.*, **30**, 1291 (1999).

Casal, J. and J. M. Martinez-Benet, "A Better Way to Calculate Cyclone Pressure Drop" *Chem. Eng.*, p. 99 (1983).

Clift, R., M. Ghadiri, and A. C. Hoffmann, "A Critique of Two Models for Cyclone Performance," *AIChE J.* **37**, 285 (1991).

Dietz, P. W., "Collection Efficiency of Cyclone Separators," *AIChE J.*, **27**, 888 (1981).

Hoekstra, A. J., J. J. Derksen, and H. E. A. Van den Akker, "A CFD Study on the Performance of a High-Efficiency Gas Cyclone," Delft Univ. of Technology Internal Report (1999a).

Hoekstra, A. J., J. J. Derksen, and H. E. A. Van den Akker,"An Experimental and Numerical Study of the Turbulent Swirling Flow in Gas Cyclones," Delft Univ. of Technology Internal Report (1999b).

Hoffmann, A. C., H. Arends, and H. Sie, "An Experimental Investigation Elucidating the Effect of Solid Loading on Cyclone Performance," *Filtr. Sep.*, **28**, 188 (1991).

Hoffmann, A. C., A. V. Santen, R. Allen, "Effect of Geometry and Solid Loading on the Performance of Gas Cyclones," *Powder Technol.*, **70**, 83 (1992).

Hoffmann, A. C., R. de Jonge, H. Arends, and C. Hanrats, "Evidence of the 'Natural Vortex Length' and Its Effect on the Separation Efficiency of Gas Cyclones." *Filt. Sep.*, **32**, 799 (1995).

Iozia, D. L. and D. Leith, "Effect of Cyclone Dimensions on Gas Flow Pattern and Collection Efficiency," *Aerosol Sci. and Technol.* **10**, 491 (1989).

Ito, S., K. Ogawa, and C. Kuroda, "Turbulent Swirling Flow in a Circular Pipe," *J. Chem. Eng. Jpn.*, **13**, 6 (1980).

Leith, D., and W. Licht, "The Collection Efficiency of Cyclone Type Particle Collectors—A New Theoretical Approach," *AIChE Symp. Ser.*, **68**, 196 (1972).

MacLean, J. P., J. D. Brown, H. D. Hoy, and J. E. Cantwell, UK Patent Application GB 2011285A (1978).

Meissner, P., and F. Löffler, "Zur Berechnung de Strömungsfeldes, im Zyklonabscheider," *Chem. Ing. Technol.*, **50**, 471 (1978).

Mothes, H., and F. Löffler, "Motion and Deposition of Particles in Cyclones," *Ger. Chem. Eng.,* **8**, 223 (1985).

Muschelknautz, E. "Design of Cyclone Separators in the Engineering Practice," *Staub-Reinhalt. Luft*, **30**, 1 (1970).

Rietema, K., "The Mechanism of the Separation of Finely Dispersed Solids in Cyclones," Proc. Symp. on Cyclones, Utrecht, The Netherlands, 46 (1958).

Shepherd, C. B., and C. E. Lapple, "Flow Pattern and Pressure Drop in Cyclone Dust Collectors," *Ind. Eng. Chem.*, **31**, 972 (1939).

Stairmand, C. J., "Pressure Drop in Cyclone Separators," *Engineering*, 409 (1949).

Svarovsky, L., "Solid-Gas Separation," *Gas Fluidization Technology*, D. Geldart, ed., Wiley, New York (1986).

Zhongli, J., W. Xiaolin and S. Minxian, "Experimental Research on the Natural Turning Length in Cyclones," *Proc. Filtech Europa '91*, Karlsruhe, The Netherlands, p. 583 (1991).

Manuscript received May 30, 2000, and revision received Dec. 4, 2000.